

# Compatibilization effect of MMA-co-GMA copolymers on the properties of polyamide 6/Poly(vinylidene fluoride) blends

Danfeng Li<sup>1</sup> · Shixin Song<sup>1</sup> · Chi Li<sup>1</sup> · Chunlei Cao<sup>1</sup> · Shulin Sun<sup>1,2</sup> · Huixuan Zhang<sup>1</sup>

Received: 23 December 2014 / Accepted: 28 April 2015 / Published online: 9 May 2015  
© Springer Science+Business Media Dordrecht 2015

**Abstract** Methyl methacrylate-co-glycidyl methacrylate copolymers (MMA-co-GMA) with different GMA contents were prepared to compatibilize the polyamide 6 (PA6) and poly(vinylidene fluoride) (PVDF) blend. The chemical reactions between the carboxyl/amino end groups of PA6 and the epoxy groups, and the good miscibility between PVDF and MMA-co-GMA were responsible for the excellent compatibilization effect. DMA results showed that the glass transition peaks of PVDF phase almost disappeared in the PA6/PVDF/MMA-co-GMA blends; this proved the suppressed thermal transition due to the restricted movement of PVDF chains. MMA-co-GMA copolymers significantly decreased the phase domain size of the PA6/PVDF blends. PVDF dispersed in the PA6 matrix uniformly and the interface between the two phases was obscure due to the compatibilization. The addition of MMA-co-GMA into the PA6/PVDF blend decreased the crystallization temperature of the PVDF phase, which proved that the compatibilizer enhanced the interaction between PVDF and PA6 and retarded the crystallization. Mechanical tests indicated that the impact strength and elongation at break of the PA6/PVDF blends increased with the addition of MMA-co-GMA. The increase of the fracture toughness was due to the compatibilization effect of MMA-co-GMA copolymers, which induced a delay

of the debonding of PA6 and PVDF phases at the interface and inhibited the initiation and propagation of cracks.

**Keywords** PA6 · PVDF · Compatibilization · MMA-co-GMA copolymer

## Introduction

Polymer blending has attracted much attention for both industrial applications and academic purposes, and provides the most versatile and economical method to prepare new polymeric materials [1, 2]. The polymer blends are usually obtained through mechanical shearing in a mixer at high temperature or by the solution blending method. However, most polymer blends are immiscible due to the large unfavorable enthalpy of mixing, resulting in the poor interfacial adhesion between the matrix phase and the dispersed phase, the inhomogeneous phase structure and the deterioration of the properties. Therefore, compatibilization is usually used to modify the miscibility, and control and stabilize a desired morphology in a polymer blend in order to generate polymeric materials with favorable properties.

Recently, polyamide6 (PA6) and poly(vinylidene fluoride) (PVDF) blends have attracted much attention [3–13]. The PA6/PVDF blends combine the good weathering resistance, chemical resistance and excellent barrier properties of PVDF and the good processability and mechanical properties of PA6. It has been found that PA6 and PVDF have favorable molecular interactions compared to other immiscible polymer blends due to the interfacial hydrogen bonds and dipolar intermolecular interactions between PA6 and PVDF [6]. Because of these molecular interactions, PA6/PVDF blends with improved properties even without compatibilization have been studied in detail by some researchers [3–6]. Na et al.

✉ Shulin Sun  
sunshulin1976@163.com

<sup>1</sup> Engineering Research Center of synthetic resin and special fiber, Ministry of Education, Changchun University of Technology, Changchun 130012, China

<sup>2</sup> Department of Chemical Engineering, Lehigh University, Bethlehem, PA 18015, USA

reported that PA6/PVDF blends achieved superior toughness with semi-crystalline PVDF components as the dispersed particles. They concluded that the transformation from  $\alpha$  to  $\beta$  phase and fibrillation of  $\beta$ -crystals of the dispersed PVDF particles were responsible for the toughness enhancement in the PA6/PVDF blend [3]. Song et al. prepared PVDF/PA6 blends via the precipitation method. They found the interfacial hydrogen bonds existing between PVDF and PA6 chain segments and the PA6 component could form a polar environment around the PVDF segment, which was conducive to the formation of the  $\beta$  phase of PVDF [4].

Despite the favorable interaction, PA6/PVDF blends are still immiscible over the entire concentration range. From research on the PA6/PVDF simple blends, it could be found that the phase domain size of the dispersed phase was still big (0.5 ~2 $\mu$ m) at some constitution such as 50/50, and the phase interface was obvious [3, 11]. In order to change the interface and improve the miscibility of PA6/PVDF blends, researchers have attempted several methods of compatibilization. Wu and Mascia prepared carboxylated polyvinylidene fluoride (PVDF-g-AAc) to modify the interface between PA6 and PVDF [8–10]. Kim et al. used poly(methyl methacrylate-co-methacrylic acid) as a compatibilizer for PA6/PVDF blends. The compatibilization mechanism was due to the chemical reaction between the carboxylic acid groups in the MAA unites and the end amino groups of PA6 forming block or graft copolymers in situ. However, Kim found that a low concentration of carboxylic acid groups and amino groups could undergo the reaction to form P(MMA-co-MAA)-g-nylon 6. The blend samples need heat treatment for 30 min at 270°C prior to molding to obtain better properties [11]. Recently, Emmanuel P. Giannelis and Yang used nano-materials, such as nanoclay and graphene oxides, as compatibilizers for PA6/PVDF blends, and detailed compatibilization mechanisms were investigated [12, 13].

In the present work, the copolymers of MMA-co-GMA with different GMA contents were prepared by a continuous solution polymerization method and were used to compatibilize PA6/PVDF blends. Compared to the chemical reaction between the carboxylic acid groups in the MAA units and the end amino groups of PA6, the reactive rate is much more rapid for the epoxy groups in the GMA units and the amino groups. MMA-co-GMA copolymers showed a much better compatibilization effect than P(MMA-co-MAA), which can be testified by morphology observations. Tensile test and

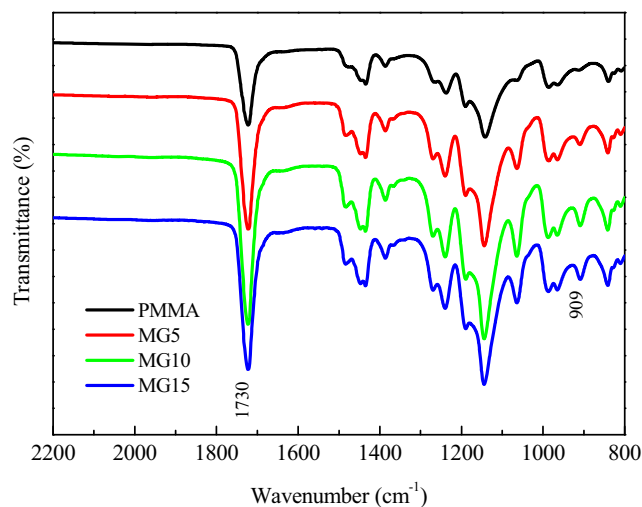


**Fig. 1** FTIR of MMA-co-GMA copolymers

scanning electron microscope (SEM) results showed that the MMA-co-GMA copolymers displayed a much better compatibilization effect than nano-clay and graphene oxides from the change of dispersed phase size and higher tensile toughness of PA6/PVDF blends. Other tests, such as DMA, DSC, SEM and FTIR have also been used to study the PA6/PVDF/MMA-co-GMA blends in detail.

## Experimental

### Materials

PVDF (Solef 6010, made in France) was purchased from Shanghai Alliedneon New Materials Co., Ltd. (Shanghai, China). The MMA-co-GMA copolymers were synthesized in

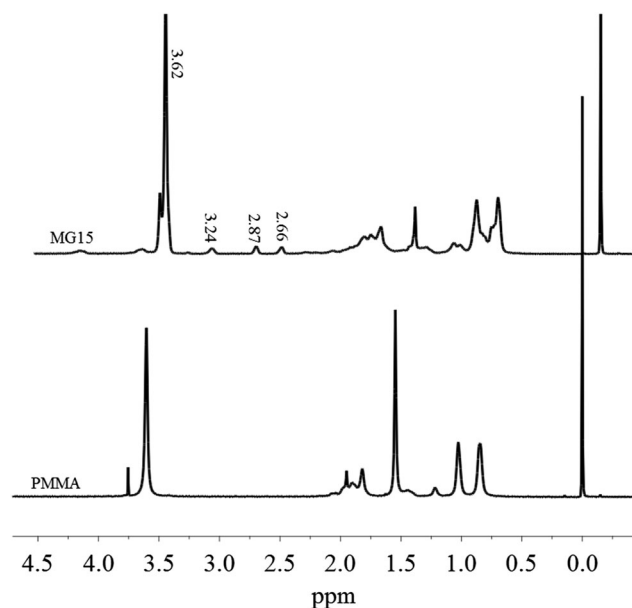


**Fig. 2**  $^1\text{H}$  NMR of PMMA and MG15 copolymer in  $\text{CDCl}_3$

**Table 1** Properties of MMA-co-GMA copolymers

Designation	GMA (wt%)	MMA (wt%)	$M_n \times 10^4$	$M_w \times 10^4$	PDI
MG5	5	95	7.2	15.84	2.2
MG10	10	90	6.9	14.49	2.1
MG15	15	85	6.6	13.20	2.0

**Table 2** Sample composition expressed as weight percentage

Designation	PA6 content (wt%)	PVDF content (wt%)	MG content (wt%)	GMA content in MG (wt%)
PA6/PVDF	50	50	0	–
PA6/PVDF/MG5	47.5	47.5	5	5
PA6/PVDF/MG10	47.5	47.5	5	10
PA6/PVDF/MG15	47.5	47.5	5	15

our lab. The MMA and GMA monomers were supplied by Jilin Chemical Industry Group Synthetic Resin Factory, China.

### Preparation of MMA-co-GMA copolymers

The MMA-co-GMA copolymers were prepared by a continuous solution polymerization method. Firstly, the reactor was pre-charged with two-thirds of the MMA/GMA/toluene/initiator mixture, and then the mixture was heated by an oil bath. The reaction temperature was 155 °C and the initiator was di-tert-butyl peroxide. When the desired reaction temperature was reached, the continuous polymerization was started. The MMA/GMA/toluene/initiator mixture was continuously injected into the reactor by a feed pump at a given rate, and at the same time, the reaction product in the reactor was continuously pumped into the twin-screw devolatilization extruder by melt pump at the same rate as the feed pump to remove the solvent and residual monomer, and then the MMA-co-GMA melt was cooled and pelletized. The properties of MMA-co-GMA copolymers are listed in Table 1.

### FTIR and NMR tests

The  $^1\text{H}$  NMR was recorded by a 400 MHz nuclear magnetic resonance (NMR) spectrometer (Bruker Instruments, model Advance III 400, Germany) at room temperature using  $\text{CDCl}_3$  as a solvent and TMS as an internal standard. Infrared spectrum was obtained on a Fourier transform infrared spectroscopy (FTIR) spectrometer (Nicolet, AVATAR-360, USA) in the 4000–400  $\text{cm}^{-1}$  range.

Figure 1 shows the FTIR spectrum curves of PMMA and MMA-co-GMA copolymers. The peak of 1730  $\text{cm}^{-1}$  represents the ester vibration of both PMMA and MMA-co-GMA. The epoxy group gives the band at 909  $\text{cm}^{-1}$  for the GMA component.  $^1\text{H}$  NMR spectroscopy was used to study the molecular structure of the prepared PMMA and MMA-co-GMA copolymers, and the results are showed in Fig. 2. The peaks at 3.24, 2.87 and 2.66 ppm belong to the H characteristic shift on the epoxy groups of GMA. The peak at 3.62 ppm is the H characteristic shift on the methoxy groups of MMA. So the FTIR and  $^1\text{H}$  NMR tests prove that MMA-co-GMA copolymers have been successfully prepared.

### Blending and processing procedures

The blending was carried out in a Thermo Haake mixer. The rotating speed was set at 55 rpm and the temperature was set at 240°C. The mixing time was 5 min. The composition of the blends is listed in Table 2. The blends were then compression molded for 5 min at 240°C to form tensile test specimens.

### DSC analysis

Perkin-Elmer DSC-7 was used to study the melting and crystallization behavior of PA6/PVDF and PA6/PVDF/MMA-co-GMA blends. The samples were heated from 30 to 240°C at 10°C/min and held for 3 min at 240°C, then cooled from 240°C to 30°C at 10°C/min. The crystallization behavior was analyzed on cooling from the melt. The tests were under a nitrogen atmosphere.

### DMA analysis

The blends were compression molded at a melting temperature of 240°C to obtain plates that were suitable for DMA test. These plates were sized 30×4×1  $\text{mm}^3$ . The sample was tested on a Perkin Elmer dynamic mechanical analyzer. The sample was heated from -80 to 80°C at a heating rate of 3°C/min and a frequency of 1Hz.

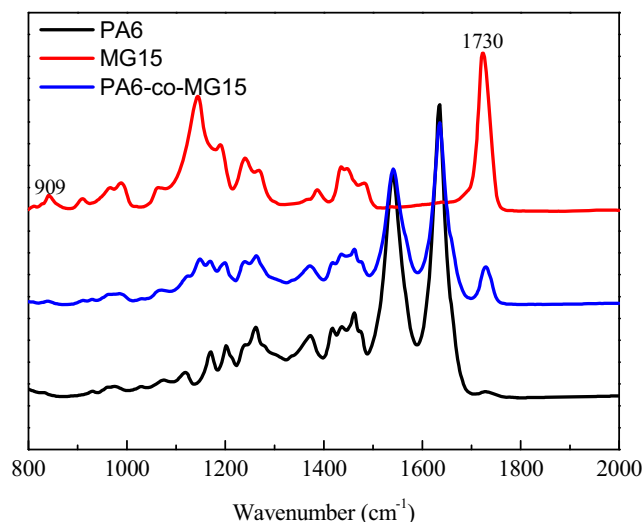
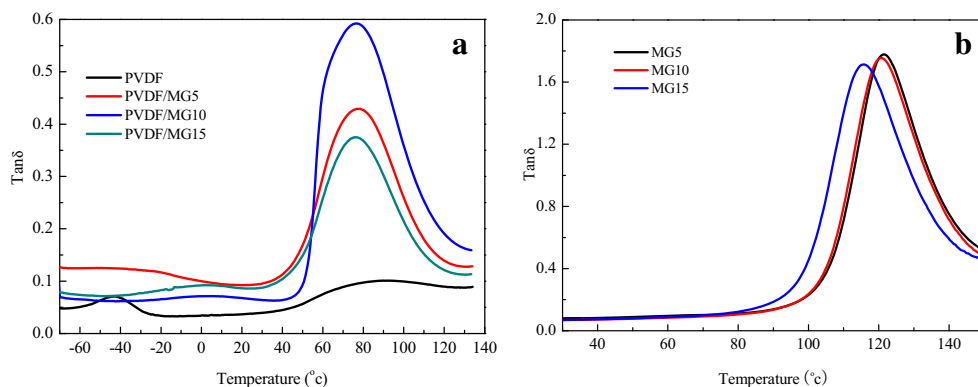


**Fig. 3** FTIR of PA6, MG15 and extracted PA6-co-MG15 copolymer

**Fig. 4** DMA curves of PVDF and PVDF/MMA-co-GMA blends



### Morphological properties

SEM micrographs were obtained with a JSM6510 scanning electron microscope (JEOL, Japan) with an operation voltage of 10 kV. Before testing, the samples were frozen in liquid nitrogen for 3 h and then fractured. The fracture surface of the samples was coated with a gold layer for SEM observation.

### Mechanical properties

The uniaxial tensile tests were carried out at  $23 \pm 2^\circ\text{C}$  on an Instron 3365 tensile tester at the cross-head speed of 5 mm/min. The specimens were cut from the compression-molded samples into dumbbell shape with the dimension of  $30 \times 4 \times 1 \text{ mm}^3$ . For the tensile tests, at least five samples with different compositions were performed.

## Results and discussion

### Compatibilization mechanisms

Most compatibilizers are commercial copolymers or are formed in situ during reactive blending through interfacial chemical reactions. Since the commercial copolymers for a particular blend may not always be available, the in situ copolymers formed during reactive blending are a better choice for compatibilization. In the present paper, MMA-co-GMA copolymers with different GMA content were blended with PA6 and PVDF. The chemical reactions between the epoxy

group of GMA and the carboxyl and amino end groups of PA6 have been used extensively to compatibilize PA6 blends [14–19]. In the present work, FTIR was used to prove the chemical reactions between PA6 and MMA-co-GMA copolymers. Figure 3 shows the FTIR of PA6, MG15, and the extracted PA6/MG15 blend. The free MG15 was extracted from the blend by tetrahydrofuran. It can be found that the characteristic peak of epoxy group at  $909 \text{ cm}^{-1}$  disappears due to the chemical reactions. The extracted PA6/MG15 blend shows the characteristic peak of a carbonyl group at  $1730 \text{ cm}^{-1}$ , which indicates that MG15 has copolymerized with PA6 and induced the formation of PA6-co-MG15.

On the other hand, the PVDF is known to be miscible with PMMA over the entire composition range due to the dipole-dipole interactions between PVDF and the carbonyl group of PMMA [20, 21]. Therefore, the MMA-co-GMA copolymers should have a good miscibility with PVDF. Figure 4 shows the DMA results of PVDF, MG copolymers and PVDF/MMA-co-GMA blends. The neat PVDF shows a  $T_g$  at  $-43^\circ\text{C}$ . As for the PVDF/MG blends, the glass transition peaks of PVDF become much wider and shift to higher temperature. The  $T_g$  of pure MG5, MG10 and MG15 copolymers are 121.5, 120.9 and  $115.7^\circ\text{C}$ , respectively. The peaks near  $76^\circ\text{C}$  show the  $T_g$  of MG copolymers, which shift to lower temperatures compared to the neat MG copolymers. Therefore, the DMA result indicates good miscibility between PVDF and MG copolymers.

Figure 5 shows the SEM morphology of PVDF/MMA-co-GMA blends. No phase separation can be found from the fracture surface. Therefore, the DMA and SEM results

**Fig. 5** SEM of PVDF/MMA-co-GMA blends

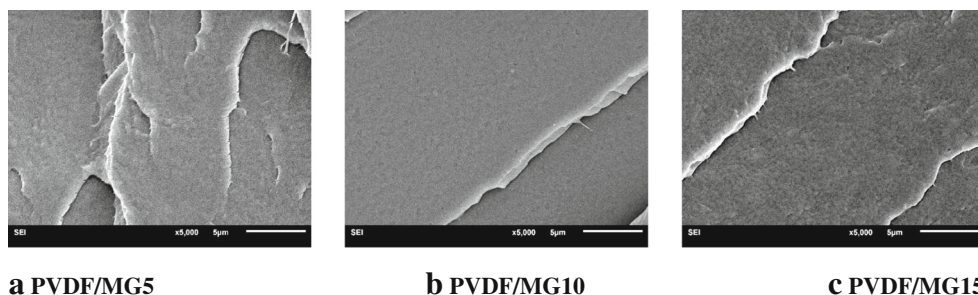
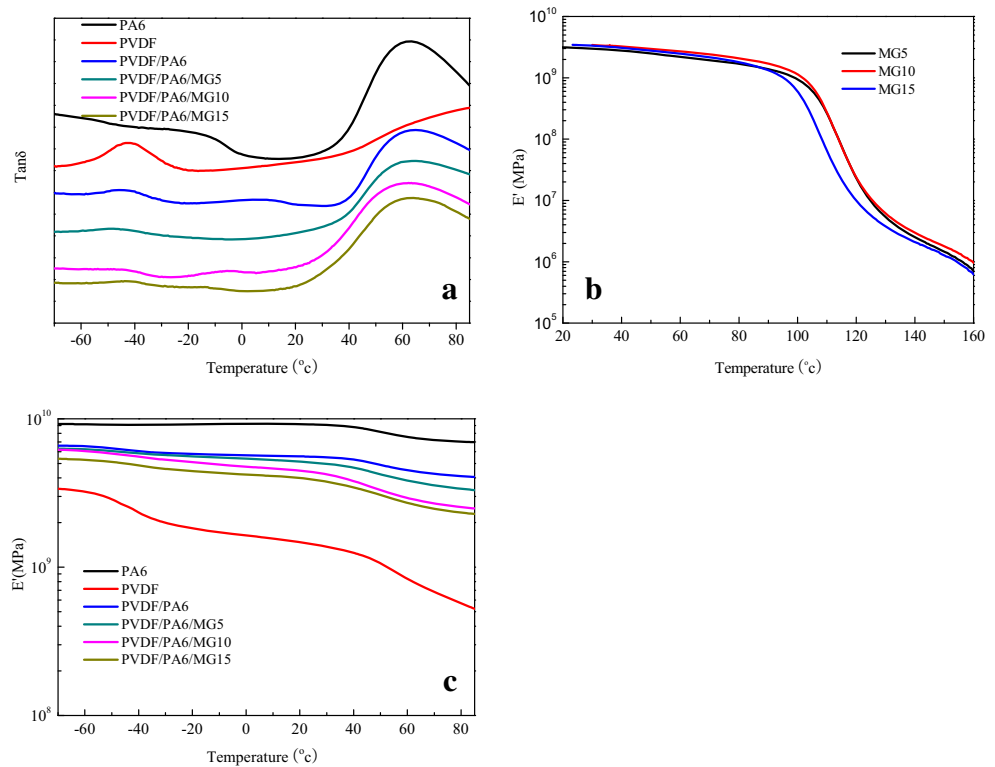




**Fig. 6** DMA curves of PA6, MG, PVDF and their blends



indicate PVDF and MMA-co-GMA copolymers have good miscibility. From the above analysis, we can conclude that the in situ formed PA6-co-MG at the interface can act as a compatibilizer between PA6 and PVDF phases.

**DMA analysis**

Figure 6a shows the Tan δ curves of PA6, MG, PVDF and their blends. The glass transition temperatures of neat PA6 and PVDF are 63°C and -43°C. As for the PA6/PVDF blend, the T<sub>g</sub> of PA6 and PVDF have almost no change compared with the neat polymers. When the MMA-co-GMA copolymers are added into the PA6/PVDF blends, the T<sub>g</sub> of PA6 phase, which is 63~64°C, still has no obvious change. However, the glass transition peaks of PVDF phase almost disappear in the PA6/PVDF/MMA-co-GMA blends, which proves the suppressed thermal transition due to the restricted movement of PVDF chains. The confinement of PVDF chains is mainly from the

smaller size in the MMA-co-GMA compatibilized PA6/PVDF blends (see Fig. 7), and similar results have been found by other research studies. Figure 6b show the E' curves of MG copolymers. It can be found that MG5, MG10 and MG15 have similar E' when the temperature is lower than the T<sub>g</sub> of MG copolymers. Figure 6c shows the E'' curves of PA6, PVDF and their blends. Compared to PVDF, PA6 shows a much higher storage modulus. The E' of PA6/PVDF blend is between the neat PA6 and PVDF. When MG copolymers were added, the E' decreased to some degree. On the other hand, with the increase of GMA content in the MG copolymers, the blends showed much lower E'. Since the MG copolymers have a similar modulus, the decrease of E' for the blends should be due to the compatibilization effect, which induces much smaller PVDF phase size and higher interfacial adhesion. The influence of PVDF on the E' of the PA6/PVDF/MG blends improves and leads to much lower E' after the low modulus of PVDF phase.

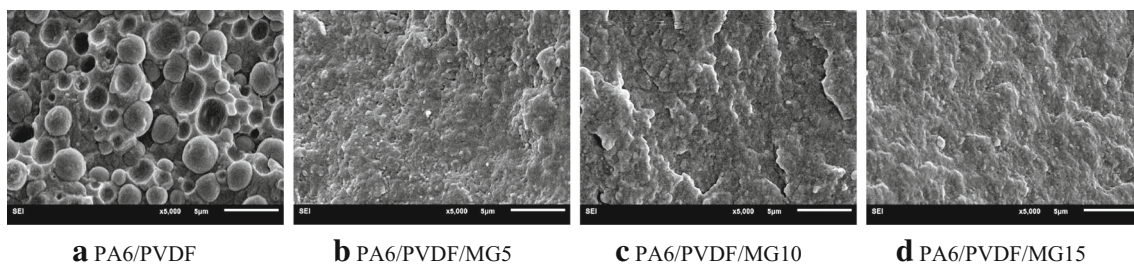
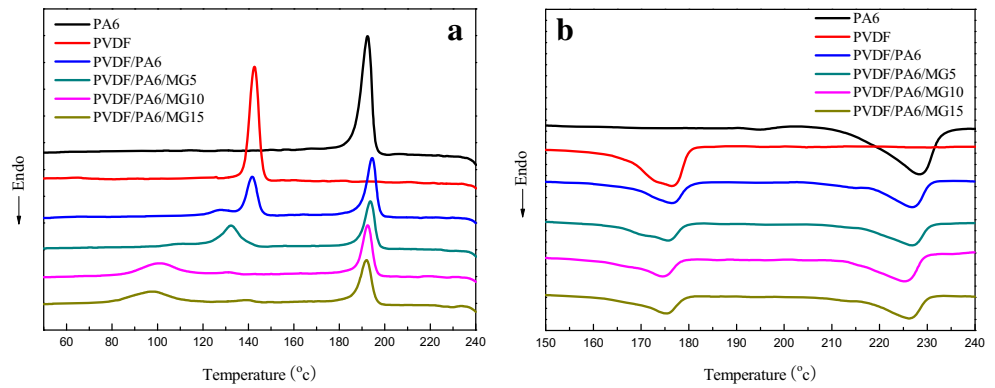


**Fig. 7** SEM morphology of PA6/PVDF and PA6/PVDF/MMA-co-GMA blends

**Fig. 8** The crystallization (a) and melting behavior (b) of PA6, PVDF and their blends



### Dispersed phase morphology

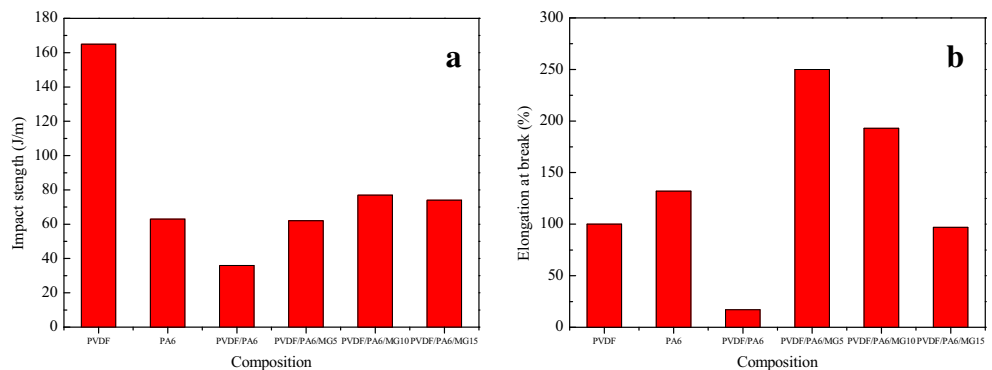
Figure 7 shows the SEM morphology of PA6/PVDF and PA6/PVDF/MMA-co-GMA blends. For the PA6/PVDF blends, the PVDF particles disperse in the PA6 matrix with discrete interface. The particle size shows a wide polydispersity from 0.2  $\mu\text{m}$  to 2  $\mu\text{m}$ . When MMA-co-GMA copolymers are added into PA6/PVDF blends, the dispersed phase morphology changes significantly. The domain size of PVDF phase decreases to 0.1–0.5  $\mu\text{m}$  and shows a uniform dispersion. The PA6 and PVDF interface becomes more diffuse due to the compatibilization effect of MMA-co-GMA copolymers. On the other hand, the higher GMA content in the MMA-co-GMA copolymers induces a better interfacial modification effect due to the higher concentration of epoxy groups and end amino/carboxyl groups undergoing the reaction to form PA6-co-MG in situ. From SEM observations, MMA-co-GMA copolymers have an excellent compatibilization effect on the PA6 and PVDF blends.

### Crystallization and melting analysis

The crystallization and melting behaviors of PA6/PVDF and PA6/PVDF/MMA-co-GMA blends were studied by DSC. As can be found from Fig. 8a, the crystallization temperatures of

neat PA6 and PVDF are 192.3°C and 142.7°C. In the PA6/PVDF blend, the crystallization temperatures of PA6 and PVDF are 194.3°C and 141.7°C, which shows a small difference with the pure components. As for the PA6/PVDF/MMA-co-GMA blends, the crystallization temperature of PA6 phase has almost no change. However, the crystallization temperature of PVDF decreases significantly, and the much higher GMA content in the MMA-co-GMA copolymers induces the lower crystallization temperature of PVDF phase. The crystallization test proves the confined crystallization of PVDF due to the smaller domain size. It is deemed that homogeneous nucleation is responsible for the confined crystallization, since the available heterogeneous nuclei in each domain are reduced significantly with decreasing of domain size. Figure 8b shows the melting behavior of PA6, PVDF and their blends. The melting temperatures of PA6 and PVDF are 228°C and 176°C. As for the PA6/PVDF blends, the melting temperature of PA6 decreases about 1.5°C and the melting temperature of PVDF has no change. When MMA-co-GMA copolymers were added, the melting temperature of PA6 and PVDF shifted to lower temperatures to some degree. Therefore, the compatibilization reactions inhibited the crystallization process of PA6 and PVDF. On the other hand, the relatively low decrease in the melting temperature suggested that the reactions between the reactive groups were not sufficient

**Fig. 9** Impact strength and elongation at break of PA6, PVDF and PA6/PVDF/MG blends



at the present processing condition. Similar results had been reported in other paper [11]. In these blends, there were no changes of the crystalline form for PVDF phase.

### Mechanical properties

Figure 9a shows the impact strength of PA6, PVDF and PA6/PVDF/MG blends. The impact strength values of PA6 and PVDF are 63 J/m and 165 J/m. However, the impact strength of PA6/PVDF blend is only 32 J/m, which is far lower than that for pure PA6 and PVDF. The PVDF has no toughening effect on the PA6 phase. With the addition of MMA-co-GMA, the impact strength of PA6/PVDF blends improves significantly. The impact strength of PA6/PVDF/MG10 blend is 77 J/m, which is a 140 % improvement compared to PA6/PVDF blends. The impact toughness improvement of PA6 with the addition of PVDF is different from the ordinary rubber-toughened PA6. For rubber-toughened PA6 blends, the rubber particles have a much lower modulus, which can cavitate during the deformation process and promote shear yielding of PA6 matrix. Shear yielding of PA6 matrix is the main energy absorption mode, and toughened PA6 shows superior toughness. However, for the PA6/PVDF blends, the cavitation of PVDF and shear yielding of PA6 can't take place due to the high modulus of PVDF. The toughening mechanisms for PVDF-modified PA6 were crystal phase transformation and fibrillation of PVDF, as discussed by Na [3]. Therefore, the toughness improvement of PA6 was not significant with the addition of PVDF.

Figure 9b shows the elongation at break of PA6, PVDF and PA6/PVDF/MG blends. The elongation at break of PA6 and PVDF is 132 % and 100 %, respectively. As for the PA6/PVDF blend, the elongation at break is just 17 %, which shows the poor fracture toughness. On the other hand, with the addition of MMA-co-GMA, the elongation at break of PA6/PVDF/MG blends increases obviously. The elongation at the break of PA6/PVDF/MG5 is 250 %, behaving as excellent ductile fracture. The decrease of elongation at break for the PA6/PVDF/MG blends at increasing GMA content in MG copolymers maybe due to the crosslinking reactions that can take place between PA6 and MG phases. For PA6 and MG blends, compatibilization and crosslinking reactions may take place. Compatibilization reactions involve the epoxy group of MG copolymers and amine and/or carboxyl groups of PA6, as discussed in the compatibilization mechanisms part. Two kinds of crosslinking reactions can occur in PA6/MG blends. One involves the secondary hydroxyl groups present on the copolymer of PA6-co-MG formed at the interface. The other is based on the bifunctionality of the PA6 matrix, as each PA6 contains two functional groups that can react with the epoxy groups. The crosslinking reactions between PA6 and MG may form defects in the PA6/PVDF/MG blends and induce the decrease of elongation at break of the blends. Similar reactions

have been found in other papers [16]. The mechanical test results show the small domain size of the dispersed PVDF phase and good interfacial adhesion between PA6 and PVDF phases are the two important reasons for toughness improvement. The increase of interfacial strength due to the compatibilization effect of MMA-co-GMA copolymers induces a delay of debonding of the PA6 and PVDF phases at the interface, and inhibits the initiation and propagation of cracks. Therefore, the toughness of PA6/PVDF blends is improved significantly.

### Conclusions

The MMA-co-GMA copolymers can effectively improve the compatibility of PA6/PVDF blends. The compatibilization mechanisms are due to the chemical reactions between the carboxyl/amino end groups of PA6 and the epoxy groups of MMA-co-GMA, and the excellent miscibility property for the PVDF and MMA-co-GMA copolymers, which have been demonstrated by the FTIR, SEM and DMA tests. The interfacial hydrogen bonds and dipolar intermolecular interactions between PA6 and PVDF are not sufficient to improve the interface properties, and the PA6/PVDF blend shows a much larger dispersed domain size, lower impact strength and elongation at break. The addition of MMA-co-GMA copolymers significantly decreased the dispersed domain size of PVDF in PA6 matrix, and the impact strength and elongation at the break of PA6/PVDF blends were improved 140 % and 1370 %, respectively. The increase of the interfacial strength and smaller domain size of PVDF in the PA6 matrix led to the confined crystallization and a lower crystallization temperature of PVDF phase, which further proved the compatibilization effect of MMA-co-GMA copolymers for the PA6/PVDF blends.

**Acknowledgments** This work was financially supported by the National Natural Science Foundation of China and Jilin Provincial Science & Technology Department under Grants 51273025, 51273026 and 201401011104JC.

### References

1. Paul DR, Bucknall CB (2000) Polymer blends: Formulation. Wiley-interscience publication, New York
2. Utracki LA (2002) Polymer blends handbook. Kluwer academic publishers, Netherlands
3. Na B, Xu WF, Lv RH, Li ZJ, Tian NN, Zou SF (2010) Toughening of nylon-6 by semicrystalline poly(vinylidene fluoride): Role of phase transformation and fibrillation of dispersed particles. *Macromolecules* 43:3911–3915
4. Song R, Liu X, Wang HF, Xia GM, He LH, Wang Y, Huang W, Zhao QL (2014) Enhanced  $\beta$  phase of polyvinylidene fluoride with

- addition of polyamide 6: role of interfacial interactions. *Colloid Polym Sci* 292:817–828
5. Liu ZH, Marechal P, Jerome R (1998) Blends of poly(vinylidene fluoride) with polyamide 6: interfacial adhesion, morphology and mechanical properties. *Polymer* 39:1779–1785
  6. Liu ZH, Marechal P, Jerome R (1997) Melting and crystallization of poly(vinylidene fluoride) blended with polyamide 6. *Polymer* 38: 5149–5153
  7. Li YJ, Shimizu H (2008) Conductive PVDF/PA6/CNTs nanocomposites fabricated by dual formation of cocontinuous and nanodispersion structures. *Macromolecules* 41:5339–5344
  8. Wu Y, Yu XB, Yang YM, Li BY, Han YC (2005) Studies on the reactive polyvinylidene fluoride-polyamide 6 interfaces: rheological properties and interfacial width. *Polymer* 46:2365–2371
  9. Mascia L, Hashim K (1997) Compatibilization of poly(vinylidene fluoride)/nylon 6 blends by carboxylic acid functionalization and metal salts formation. 1. Grafting reactions and morphology. *J Appl Polym Sci* 66:1911–1923
  10. Mascia L, Hashim K (1998) Compatibilization of poly(vinylidene fluoride)/Nylon 6 blends by carboxylic acid functionalization and metal salts Part 2. Mechanism and effects on physical. *Polymer* 39: 369–378
  11. Kim KJ, Cho HW, Yoon KJ (2003) Effect of P(MMA-co-MAA) compatibilizer on the miscibility of nylon 6/PVDF blends. *Eur Polym J* 39:1249–1265
  12. Loan TV, Emmanuel PG (2007) Compatibilizing poly(vinylidene fluoride)/nylon-6 blends with nanoclay. *Macromolecules* 40:8271–8276
  13. Yang JH, Feng CX, Dai J, Zhang N, Huang T, Wang Y (2013) Compatibilization of immiscible nylon6/poly(vinylidene fluoride) blends using graphene oxides. *Polym Int* 62:1085–1093
  14. Filippi S, Yordanov H, Minkova L (2004) Reactive compatibilizer precursors for LDPE/PA6 blends, 4(a) Maleic anhydride and glycidyl methacrylate grafted SEBS. *Macromol Mater Eng* 289:512–523
  15. Wei Q, Chionna D, Galoppini E (2003) Functionalization of LDPE by melt grafting with glycidyl methacrylate and reactive blending with polyamide-6. *Macromol Chem Phys* 204:1123–1133
  16. Sun SL, Tan ZY, Xu XF, Zhou C, Ao YH, Zhang HX (2005) Toughening of nylon-6 with epoxy-functionalized acrylonitrile-butadiene-styrene copolymer. *J Polym Sci Polym Phys* 43:2170–2180
  17. Sun SL, Chen ZC, Zhang HX (2008) Effect of reactive group types on the properties of core-shell modifiers toughened PA6. *Polym Bull* 61:443–452
  18. Tjong SC, Meng YZ (2004) Structural-mechanical relationship of epoxy compatibilized polyamide 6/polycarbonate blends. *Mater Res Bull* 39:1791–1801
  19. Hema S, Neeraj KG (2011) Evolution of properties in ABS/PA6 blends compatibilized by fixed weight ratio SAGMA copolymer. *J Polym Res* 18:1365–1377
  20. Song HH, Yang SJ, Sun SL, Zhang HX (2013) Effect of Miscibility and Crystallization on the Mechanical Properties and Transparency of PVDF/PMMA Blends. *Polym Plast Technol* 52:221–227
  21. Pawde SM, Deshmukh K (2009) Investigation of the structural, thermal, mechanical, and optical properties of Poly(methyl methacrylate) and Poly(vinylidene fluoride) blends. *J Appl Polym Sci* 114: 2169–2179